Urban heat island impacts on plant phenology: intra-urban variability and response to land cover

2016 Environ. Res. Lett. 11 054023

(http://iopscience.iop.org/1748-9326/11/5/054023)

Environmental Research Letters

LETTER

Urban heat island impacts on plant phenology: intra-urban variability and response to land cover

Samuel C Zipper[1,2,6], **Jason Schatz**[3], **Aditya Singh**[4], **Christopher J Kucharik**[3,5], **Philip A Townsend**[4] **and Steven P Loheide II**[1,2]

[1] Freshwater & Marine Sciences Program, University of Wisconsin-Madison, Madison WI, USA
[2] Department of Civil & Environmental Engineering, University of Wisconsin-Madison, Madison WI, USA
[3] Department of Agronomy, University of Wisconsin-Madison, 1575 Linden Drive, Madison WI 53706, USA
[4] Department of Forest and Wildlife Ecology, University of Wisconsin-Madison, 1630 Linden Drive, Madison WI 53706, USA
[5] Center for Sustainability and the Global Environment, University of Wisconsin-Madison, Madison WI, USA
[6] Author to whom any correspondence should be addressed.

E-mail: szipper@wisc.edu **and** samuelczipper@gmail.com

Keywords: urban heat island, vegetation phenology, sensor network, urban ecology, remote sensing, land surface phenology, urban climate

Supplementary material for this article is available online

OPEN ACCESS

RECEIVED
7 December 2015

REVISED
19 April 2016

ACCEPTED FOR PUBLICATION
29 April 2016

PUBLISHED
20 May 2016

Abstract

Despite documented intra-urban heterogeneity in the urban heat island (UHI) effect, little is known about spatial or temporal variability in plant response to the UHI. Using an automated temperature sensor network in conjunction with Landsat-derived remotely sensed estimates of start/end of the growing season, we investigate the impacts of the UHI on plant phenology in the city of Madison WI (USA) for the 2012–2014 growing seasons. Median urban growing season length (GSL) estimated from temperature sensors is ~5 d longer than surrounding rural areas, and UHI impacts on GSL are relatively consistent from year-to-year. Parks within urban areas experience a subdued expression of GSL lengthening resulting from interactions between the UHI and a park cool island effect. Across all growing seasons, impervious cover in the area surrounding each temperature sensor explains >50% of observed variability in phenology. Comparisons between long-term estimates of annual mean phenological timing, derived from remote sensing, and temperature-based estimates of individual growing seasons show no relationship at the individual sensor level. The magnitude of disagreement between temperature-based and remotely sensed phenology is a function of impervious and grass cover surrounding the sensor, suggesting that realized GSL is controlled by both local land cover and micrometeorological conditions.

1. Introduction

The urban heat island (UHI) effect is characterized by elevated temperatures in urban areas, relative to the surrounding countryside (Oke 1973, 1982, 1988). Though 60% of global population is expected to live in urban areas by the year 2030, the ecological impacts of the UHI remain poorly understood (Cohen 2006, Jochner and Menzel 2015). UHI-induced increases in temperature can affect plant phenology (the timing of developmental events such as leaf emergence and senescence) both within and around cities (Jochner *et al* 2012, Jochner and Menzel 2015). Understanding the UHI influence on phenology is critical, as the start of the growing season (SOS), end of the growing season (EOS), and total growing season length (GSL) can have substantial impacts on water, energy, and carbon exchange, which in turn have important feedbacks with climate (Penuelas *et al* 2009, Richardson *et al* 2013, Keenan *et al* 2014). UHI-induced changes in GSL have direct impacts on global food security, as 25%–30% of global urban residents, most commonly from the poorest sectors of the population, are involved in food production and 60% of irrigated agriculture (35% rainfed) is within 20 km of urban areas (Orsini *et al* 2013, Thebo *et al* 2014). Moreover, UHI-driven advances in spring may compound shifts in GSL that are already occurring due to climate

change (Menzel and Fabian 1999, Schwartz and Reiter 2000) and thus increase the survival and activity of harmful insects and pathogens (Bradley and Altizer 2007).

Numerous observational studies have reported urban–rural phenological differences in Africa (Gazal *et al* 2008), Europe (Menzel and Fabian 1999, Roetzer *et al* 2000, Gazal *et al* 2008, Jochner *et al* 2012, Comber and Brunsdon 2015), Asia (Omoto and Aono 1990, Gazal *et al* 2008, Jeong *et al* 2011), and North America (Primack *et al* 2004, Gazal *et al* 2008, Neil *et al* 2010). These studies primarily select one or several species to monitor phenology at discrete points and are not designed to capture variability within urban areas (Mimet *et al* 2009, Fotiou *et al* 2011, Comber and Brunsdon 2015). While sensor networks are widely used to describe UHIs (see Schatz and Kucharik 2014 for a summary of previous work), very few studies have investigated the spatial variability of UHI effects on GSL (Todhunter 1996, Smoliak *et al* 2015).

Due to the difficulty in studying phenological variability from the ground, satellite remote sensing is often used to study spatial variability in GSL to understand the impacts and extent of the UHI. For example, White *et al* (2002), Zhang *et al* (2004), Fisher *et al* (2006), and Elmore *et al* (2012) found increases in GSL ranging from 0 to 15 d associated with urban areas in the eastern USA, with a zone of influence extending up to 32 km from the urban margin. However, each of these studies relies on either masking out urban areas to study exclusively deciduous forest in or near urban areas or uses satellite data so coarse in resolution that spatial heterogeneity is obscured. These limitations reduce our ability to explore drivers of GSL within urban areas, where the impacts of UHIs on phenology would likely be both strongest and most variable.

In this study, we combine a network of temperature sensors of near unprecedented density and extent (Schatz and Kucharik 2014, Smoliak *et al* 2015) with Landsat-derived phenological metrics at 30 m resolution to study fine-scale degree day-based and remotely sensed response of SOS, EOS, and GSL to the UHI both within and around Madison WI (USA). Specifically, we answer two questions: (1) how do UHI impacts on GSL vary spatially and temporally within cities?; and (2) how does remotely sensed GSL (GSL_R) compare to GSL as defined by temperature-based metrics (GSL_T)? These questions address two critical knowledge gaps in urban phenological research: the unknown influence of urban composition on phenology (Jochner *et al* 2012, Walker *et al* 2015) and how well satellite-derived estimates of growing season land surface phenology compare to ground-based micrometeorological observations (Cleland *et al* 2007, Fisher *et al* 2007, Penuelas *et al* 2009, Fu *et al* 2014b, Jochner and Menzel 2015).

2. Methods

2.1. Study area

Our study domain is Dane County (WI, USA), at the center of which is the city of Madison. Madison is a mid-sized urban area located in north-central United States (43°N, 89°W) with a population of 233 000 and an estimated urban agglomeration population of 402 000 (US Census Bureau 2010). The climate is humid continental, characterized by consistently below-freezing winter temperatures and warm summers with precipitation dominated by convection-based storms. Madison is surrounded by an agricultural landscape intermingled with deciduous forest and lakes (figure 1(a)).

2.2. Sensor data

Beginning in March 2012, 151 HOBO U23 Pro v2 temperature/RH sensors (Onset Computer Corporation, Bourne MA) were installed on utility and streetlight poles in and around Madison. 135 sensors were installed in March 2012, with an additional six sensors installed in October 2012 and ten more in August 2013. All sensors were equipped with radiation shields, installed at a height of 3.5 m, and logged instantaneous temperature every 15 min. Sensors were classified as Urban, Rural, Park, Lake, or Wetland at the time of installation. Specifically, urban sensors were defined as within the municipal limits of one of the cities or towns within the Madison metropolitan area (including Madison, Monona, Middleton, Sun Prairie, Fitchburg, Verona, Waunakee, and Stoughton), while rural sensors were outside of these boundaries. Park sensors were within municipal boundaries of a city or town, and inside an officially designated park; parks range in size from 1.7 to 520 ha, with a mean (median) size of 101 ha (39.2 ha). A full description of the sensor network, which is one of the most spatially dense and extensive in existence, can be found in Schatz and Kucharik (2014).

A detailed description of our approach for estimating SOS/EOS based on temperature data is described in appendix S1. In short, we used a heating and cooling degree day (HDD and CDD) approach developed by Richardson *et al* (2006) for sugar maple, which is the Wisconsin state tree and an important component of Madison's urban canopy. The HDD/CDD approach is based on the concept of thermal time and estimates the start and end of growing seasons based on cumulative temperature above/below a physiologically meaningful threshold (Cannell and Smith 1983, Fu *et al* 2014a).

As this approach represents only a single species and was developed in New Hampshire, we also used a permutation-based approach to quantify uncertainty associated with our estimate, in which temperature thresholds and other necessary parameters are

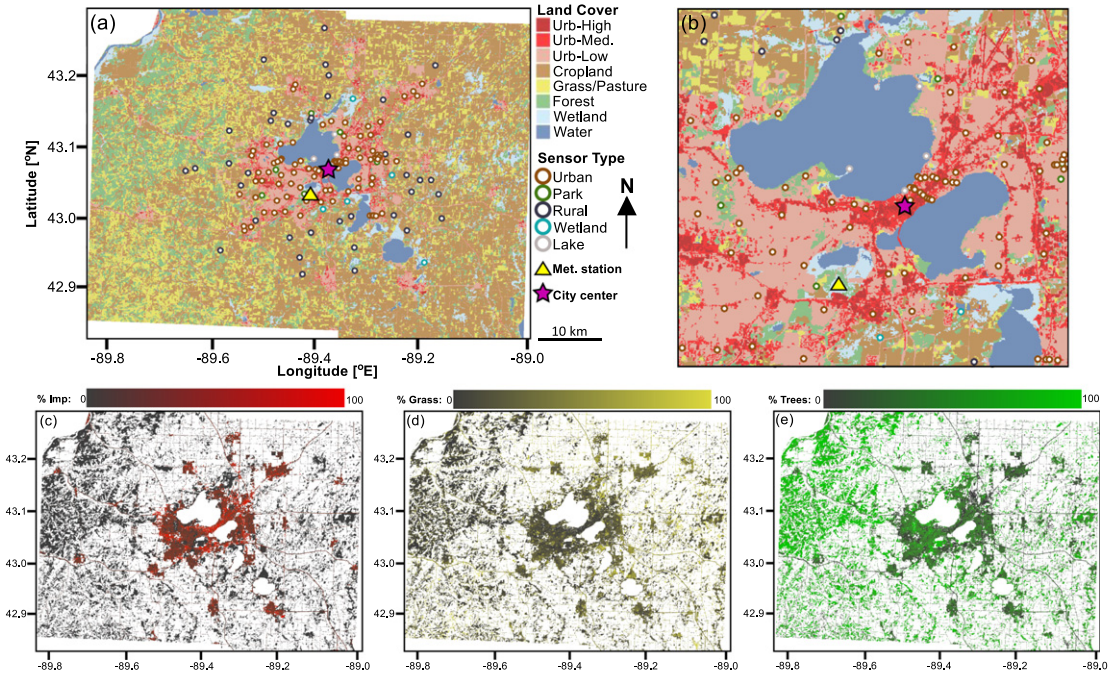

Figure 1. Map of the study area, Dane County WI. (a) NLCD land cover classification (Fry *et al* 2011), including sensor locations. (b) Close-up of Downtown Madison. (c)–(e) results of spectral unmixing analysis for % impervious, grass, and trees, respectively, calculated using the hybrid technique. Agricultural land use (cropland and grass/pasture), water and 2001–2011 land cover change are masked from (c) to (e).

randomly selected from a distribution in order to provide a range of values, from which both a mean and uncertainty can be estimated (Serbin *et al* 2014, Zipper and Loheide 2014). We selected a uniform distribution from −0.6 °C to 4 °C as our temperature threshold range for SOS thresholds for HDD accumulation, as this interval encompasses a range of vegetation, from cold-tolerant to warm-season, and these temperatures have been demonstrated as effective phenological predictors previously (Schwartz and Marotz 1986, Richardson *et al* 2006). As less data exists for the autumn phenological triggers, we varied our EOS threshold for CDD accumulation over the same 4.4 °C range centered on the 20 °C value reported by Richardson *et al* (2006) as most effective for sugar maple.

For each sensor and each growing season, cumulative HDDs beginning January 1 and CDDs beginning August 15 were used to identify the temperature-based SOS/EOS (SOS_T and EOS_T, respectively), and GSL_T was calculated as $EOS_T - SOS_T$. The 2012 SOS_T is an exception to this, as the sensors were installed in late March and therefore temperature from a meteorological station at the University of Wisconsin-Madison Arboretum were adjusted for the UHI effect unique to each sensor and used prior to March 27. Differences between urban, park, and rural sensor classes were tested for statistical significance using a pairwise t-test with significance defined as $p < 0.05$.

2.3. Satellite data

A detailed description of the methodology for calculating phenology from remotely sensed data is presented in appendix S2. We collected all Landsat images of Madison WI (path 24, row 30) over the period 2003–2013 with < 40% cloud cover, for a total of 110 images (figure S1). Each image was atmospherically corrected using the LEDAPS toolchain (Masek *et al* 2006), cloud-masked using the FMASK utility (Zhu and Woodcock 2012), and clipped to the boundaries of Dane County. We used a double-logistic model (Zhang *et al* 2003, Fisher *et al* 2006) to calculate a composite remotely sensed SOS/EOS (SOS_R/EOS_R) based on five different vegetation indices and calculated GSL_R as $EOS_R - SOS_R$.

It is important to note that this timestacking method produces a representative or average $SOS_R/EOS_R/GSL_R$ for the period 2003–2013 at each pixel, rather than $SOS_R/EOS_R/GSL_R$ for each individual growing season (Fisher *et al* 2006, Elmore *et al* 2012, Melaas *et al* 2013). Due to infrequent Landsat overpasses (figure S1) and common summer cloud cover in the area, using Landsat imagery over a smaller time period such as 2012–2014 for direct comparison with temperature-based method is not possible. However, satellites with more frequent overpasses (e.g. MODIS, AVHRR) have spatial resolutions an order of magnitude coarser, which would make studying the fine-scale impacts of the UHI on phenology impossible. While data fusion from multiple sensors shows promise at obtaining phenological estimates at high

spatial and temporal resolution (e.g. Liang *et al* 2014), fusion approaches currently struggle when pixels have a mix of land cover types, and therefore are not well-suited to urban analysis (Walker *et al* 2012, Zhang *et al* 2013, Klosterman *et al* 2014).

To address potential problems associated with comparing 2003–2013 remotely sensed imagery with 2012–2014 temperature data, all pixels containing land use change between 2001 and 2011 (Jin *et al* 2013) were masked from analysis. Furthermore, we separately fit and estimated phenology using data from the complete Landsat period of record (1982–2013) and carried out all subsequent analysis to determine whether choice of the Landsat period has an impact on results. Only results using the 2003–2013 Landsat imagery are presented here, as using 1982–2013 data did not substantially impact either results or interpretation (data not shown).

2.4. Comparison between temperature-based and remotely sensed approaches

To compare remotely sensed and temperature-based phenology, we averaged SOS_R, EOS_R, and GSL_R within a 500 m buffer surrounding each sensor, as this distance has been recommended as a zone of influence for sensor-based studies (Oke 2006) and previous work found that 500 m best describes local climate variability in our study area (Schatz and Kucharik 2014). Due to the different time periods of remotely sensed (2003–2013) and temperature-based (2012–2014) methods, it is important to note that a 1:1 relationship of phenological indicators between the methods is not expected, as the temperature regime controlling the timing of SOS/EOS varies interannually. However, temperature-based results show a consistent year-to-year relationship between SOS_T/EOS_T and impervious cover (discussed in section 3.1), indicating that the spatial patterns of UHI impact on meteorological conditions conducive to plant growth are consistent from year-to-year. Therefore, we hypothesize that a positive correlation reflecting these patterns exists between SOS_T/EOS_T from individual growing seasons and long-term average SOS_R/EOS_R. Our analysis focuses on the correlation and slope of the relationship between remotely sensed and temperature-based methods rather than bias between the two methods, as bias likely reflects the unique characteristics of the 2012–2014 growing seasons compared to the 2003–2013 average (see Ault *et al* 2013).

As a first-order attempt to quantify the impact of land cover on differences between remotely sensed and temperature-based growing season, we define three difference metrics. For each difference metric, a positive value indicates that remotely sensed estimates correspond to a longer growing season than would be predicted from meteorological data (e.g. $SOS_R < SOS_T$, $EOS_R > EOS_T$, and $GSL_R > GSL_T$):

$$(1)\ SOS_{Diff} = SOS_{T\_Norm} - SOS_{R\_Norm}$$

$$(2)\ EOS_{Diff} = EOS_{R\_Norm} - EOS_{T\_Norm}$$

$$(3)\ GSL_{Diff} = GSL_{R\_Norm} - GSL_{T\_Norm}$$

To account for the different temperature-based growing seasons (2012–2014) within a single model, we calculated normalized values of SOS_T, EOS_T, and GSL_T (denoted SOS_{T_Norm}, EOS_{T_Norm}, and GSL_{T_Norm}) by subtracting the yearly mean value across all sensors from each individual sensor's value, thus centering our data at 0 for all years. Similarly, we subtracted the overall mean value from each sensor's value for the remotely sensed metrics SOS_R, EOS_R, and GSL_R to estimate SOS_{R_Norm}, EOS_{R_Norm}, and GSL_{R_Norm}. Using this technique, there are three difference metrics for each sensor (once for each growing season).

To account for potential impacts of land use change across the interval over which Landsat results were averaged, we eliminated from analysis all pixels classified as changing land cover between 2001 and 2011 in the National Land Cover Dataset (NLCD) (Jin *et al* 2013). Furthermore, we repeated our analysis using SOS_R and EOS_R derived from a different Landsat time window (1982–2013) to check for the impacts of time domain selection on mean phenology, which had no substantial difference in results or interpretation (only 2003–2013 results shown below).

2.5. Land cover composition

We used two approaches to characterize the relative composition of impervious, tree, and grass cover at 30 m resolution (figures 1(b)–(d), both relying on spectral mixture analysis. Spectral mixture analysis is a widely used technique for estimating relative composition of different land cover classes by comparing the spectral signature of each pixel to spectra from user-defined reference endmembers (Small 2001, Wu and Murray 2003, Wu 2004, Buyantuyev *et al* 2007, Weng 2012). Inputs to both approaches were 30 cloud-free Landsat images collected between 2003 and 2013 with cropland and water masked (Gan *et al* 2014), and spectral mixture analysis was conducted in ENVI 5.0 (Exelis Visual Information Solutions, Boulder, Colorado) and constrained to a unit sum.

In the first approach (referred to as the SMA method), we performed a linear spectral mixture analysis, trained with areas of homogeneous cover manually selected in each of the three classes. In the second approach (referred to as the hybrid method), we use percent impervious cover from the NLCD (Xian *et al* 2011), a national-level impervious cover estimate widely used in the UHI literature (e.g. Georgescu *et al* 2012, 2013, Zhang *et al* 2014, Walker *et al* 2015, Schatz and Kucharik 2015, 2016). We then used spectral mixture analysis to differentiate between tree and

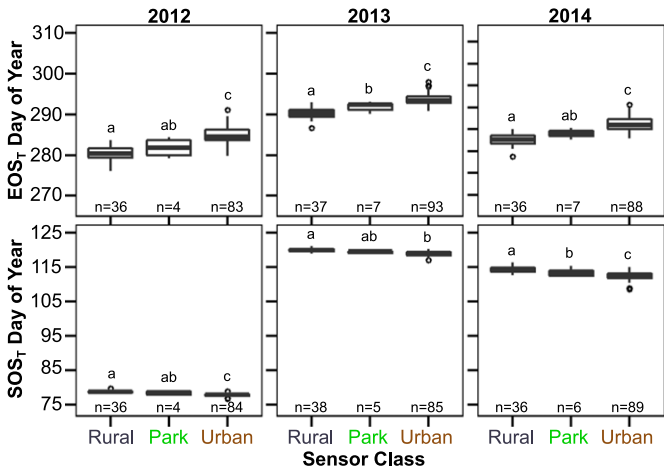

Figure 2. SOS$_T$ and EOS$_T$ based on degree-day technique aggregated by sensor class. Hinges are at the class median, boxes span the interquartile range (IQR), and whiskers span 1.5*IQR with outliers plotted as circles. Letters above boxes indicate statistically significant differences ($p < 0.05$) tested using pairwise t-test.

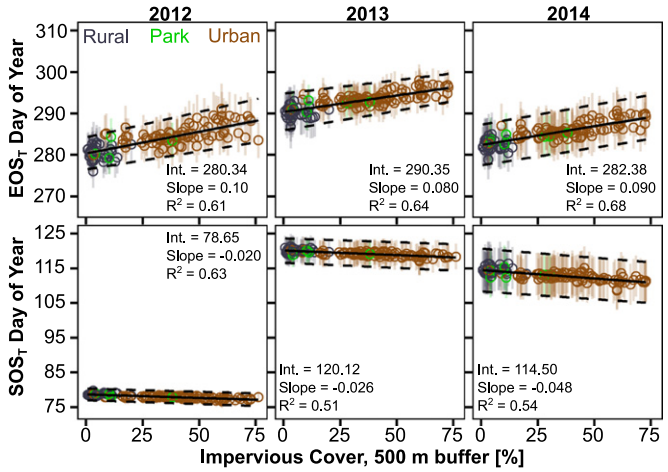

Figure 3. SOS$_T$ and EOS$_T$ based on degree-day technique, plotted as a function of impervious cover in the 500 m surrounding the sensor calculated using the hybrid method. Colors correspond to sensor type categories as shown in upper left panel. Points represent mean of 100 permutations and vertical lines one standard deviation around each point. Solid black line is a linear fit to means and dashed lines to ±1 standard deviation. All slopes and intercepts are significantly different from 0 ($p < 0.05$) using two-tailed t-test.

grass cover for the remaining percent land cover in each pixel not accounted for by NLCD impervious estimates.

We assessed the accuracy of each method by comparing results to manually digitized 2013 Dane County imagery from the US Department of Agriculture's National Agricultural Imaging Program (NAIP). NAIP imagery was manually classified into 'birds-eye view' percent impervious, tree, and grass cover at 50 randomly selected 90 m × 90 m blocks, which were compared to 3 pixel-square blocks of Landsat-derived land cover (Wu and Murray 2003, Wu 2004, Gan *et al* 2014). Comparison between the two methods revealed only minor differences in results which did not alter overall interpretation, but a slightly better performance of the hybrid method; thus, results and analysis based on the hybrid method are reported in the main body text. Accuracy assessment results and a comparison of the two methods is presented in appendix S3.

3. Results and discussion

3.1. Temperature-based growing season

The temperature-based growing season shows a strong influence of the UHI (figures 2 and 3). Median urban sensor SOS$_T$ is advanced by 0.8, 0.9, and 2.0 d relative to the rural sensors in 2012, 2013, and 2014, respectively, and urban EOS$_T$ delayed by 4.2, 3.2, and 3.3 d. These changes in SOS$_T$ and EOS$_T$ lead to a statistically significant median increase in GSL$_T$ by 4.9–5.3 d in urban areas (figure 2).

The changes in SOS$_T$ and EOS$_T$ are related most strongly to the percent impervious land surface cover (%I), a proxy for the density of the built environment, in the area surrounding the sensor (figure 3). We

averaged %I within 500 m of each sensor, as local climate variability in our study area is best described at this distance (Schatz and Kucharik 2014), but changes in buffer radius (100–1000 m) do not substantially alter results (data not shown). Across all years, R^2 for the %I–SOS_T/EOS_T relationships range from 0.51 to 0.68, indicating that physical urban density consistently explains over half of GSL_T variability. Uncertainty estimates generated using our permutation-based approach show similar trends as a function of impervious cover, indicating that variability in temperature thresholds or degree day accumulation intended to represent a range of potential urban species does not alter the relationship between the UHI and phenology.

Phenological shifts when considering rural and urban endmembers, which we define as the minimum (0.7%) and maximum (76.1%) observed impervious cover within a 500 m buffer of all sensors, were even more extreme than shifts in median SOS_T/EOS_T. The urban endmember SOS_T was advanced by 1.5–3.7 d and EOS_T delayed by 6.0–7.9 d relative to the rural endmember. This represents a potential UHI-driven extension of the growing season by 8.0–10.5 d, or 4.7%–6.2% across our three study years.

The magnitude of UHI-driven changes in phenology are strongly determined by the prevailing weather conditions during seasonal transitions. The 2012 and 2014 SOS_T provide a useful contrast to explore this dynamic. In 2012, much of the US including Madison WI experienced anomalously high late winter temperatures leading to a record-setting 'false spring' (Ault *et al* 2013). This was driven by a regional, synoptic-scale warm front which elevated temperatures above physiologically important thresholds more or less simultaneously across urban and rural parts of our study area, and therefore the small temperature differences caused by the UHI had relatively little effect. In contrast, 2014 experienced a relatively cool spring, which meant that small (1 °C to 2 °C) increases in temperature due to the UHI were able to contribute a larger proportion of the degree day requirements to trigger the onset of spring. Therefore, the magnitude of urban impacts on SOS_T were ~2.4 times as strong in 2014 compared to 2012, as measured by the difference in slopes between the two growing seasons (− 0.020 d/% in 2012 and − 0.048 d/% in 2014). This indicates that studies reporting UHI-driven increases in GSL on the basis of a single growing season (e.g. Schmidlin 1989, Zhang *et al* 2004) may not be generalizable across time without considering prevailing weather conditions during spring and fall transition periods.

Park sensors tended to have intermediate values of SOS_T and EOS_T between the urban and rural sensors, indicating that they likely experience both a UHI effect elevating temperatures above the rural surroundings and a park cool island (PCI) effect reducing temperature relative to their urban surroundings (Taha *et al* 1991, Spronken-Smith and Oke 1999, Upmanis and Chen 1999, Spronken-Smith *et al* 2000, Yu and Hien 2006, Feyisa *et al* 2014). The PCI leads to a subdued expression of the UHI and median park GSL_T 1.7–3.2 d longer than rural sensors ($p < 0.05$ in 2013 and 2014) and 1.5–3.3 d shorter than urban GSL_T ($p < 0.01$ all years). This subdued phenological response to the UHI in parks may be particularly beneficial for native and migratory species which rely on vegetation phenological events for survival (e.g. budburst), as urban parks are often viewed as refugia for species threatened by the urbanization process (Dobrowski 2011, Stagoll *et al* 2012).

3.2. Remotely sensed growing season

SOS_R, EOS_R, and GSL_R are shown in figures 4(a), (c), (e). Patterns of urban and peri-urban land surface phenology are consistent with those observed in other studies, with earlier SOS_R and later EOS_R observed close to the center of the city (Fisher *et al* 2006). Due to the elimination of agricultural lands surrounding Madison from analysis, phenological estimates are much less dense outside the urban margin. However, it is evident that GSL_R is shorter in rural landscape surrounding Madison, with several patches of longer GSL_R corresponding to small outlying cities and towns. Areas that are predominantly wetland (e.g. northeast and south of Madison) have the shortest observed GSL_R within our study domain, indicating that the growing season of naturally cool areas is well captured.

At the county scale, GSL_R increases of ~10–25 d are observed within ~10 km from the city center (defined as the Wisconsin state capitol building; purple star in figure 4(e)) and maximum increases occur ~2–7 km from the city center (figure 4(f); purple circles in figure 4(e)). These patterns exist due to the combined effects of the Madison lakes (suppressing GSL_R within 2 km of the city center) and the urban–rural transition (occurring ~6.5–11 km from the city center).

We believe that GSL_R is suppressed within the 2 km closest to the city center due to a unique characteristic of Madison, which is that the densest parts of the city are on an isthmus between two lakes (figure 1). While these lakes visually dominate the landscape, previous work by Schatz and Kucharik (2014) has found that the lake's zone of influence on temperature is relatively small (100s of meters), and impacts of lakes on temperature decay exponentially with distance from the lakeshore. Therefore, the 2 km closest to the city center (equal to the half-length of the isthmus and shown as the inner purple circle in figure 4(e)) represents the area over which lakes contribute a larger proportional influence on temperature and phenology; however, previous work has shown the influence of the lakes on temperature is minor

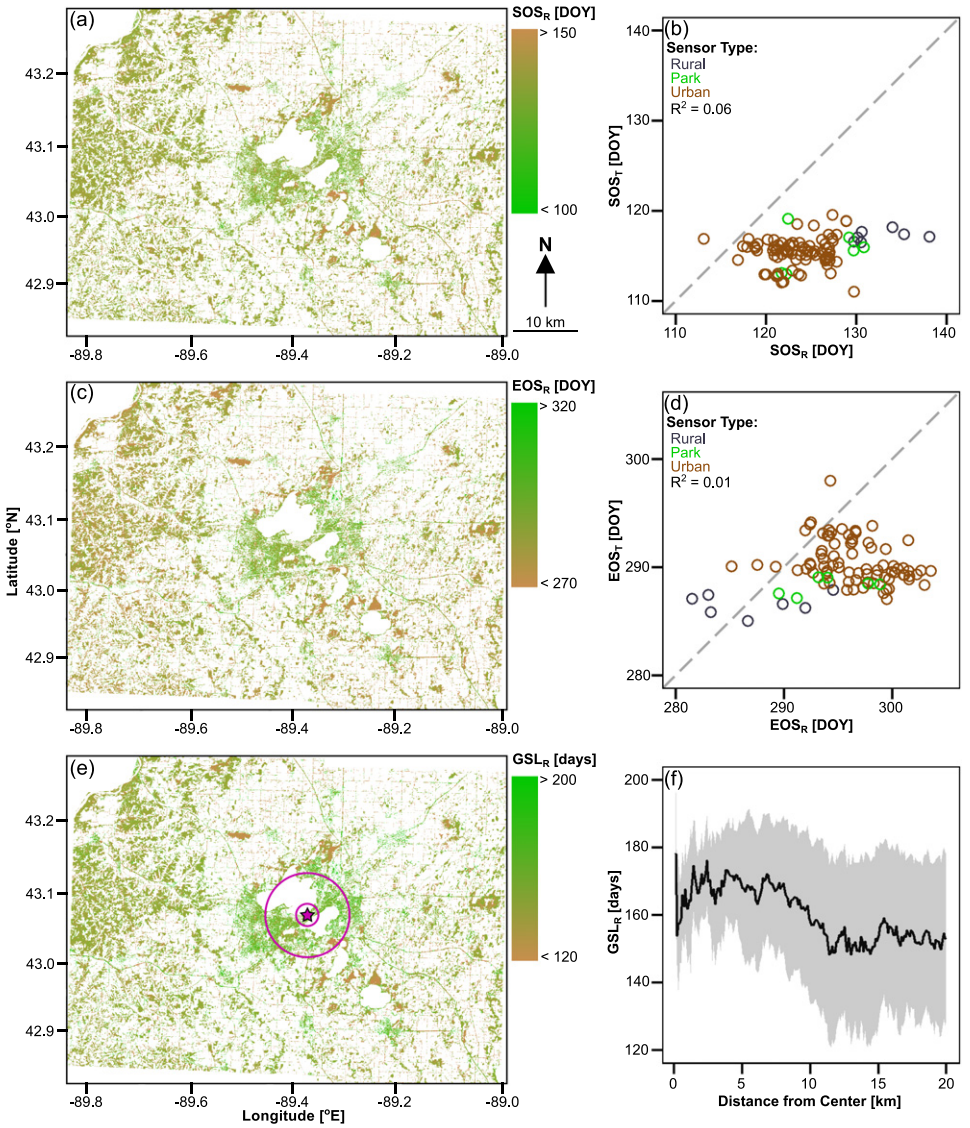

Figure 4. Remotely sensed estimates of (a) SOS_R, (c) EOS_R, and (e) GSL_R with all agriculture, water, and failed fits masked (white areas). (b) and (d) compare SOS_R to SOS_T and EOS_R to EOS_T, respectively. In (b) and (d), SOS_R and EOS_R points represent the average SOS/EOS in a 500 m buffer surrounding the sensor as described in appendix S2; SOS_T and EOS_T represent the mean of the SOS/EOS from the 2013 and 2014 growing seasons at each sensor (2012 excluded due to false spring). (f) shows GSL_R as a function of distance from the city center, which is noted as a purple star in (e). Purple circles in (e) represent 2 km (inner) and 7 km (outer) from city center. Black line in (f) represents the mean and gray shading one standard deviation of all pixels a given distance from center.

outside of this narrow zone on the isthmus (Schatz and Kucharik 2014).

Instead, the urban–rural transition represents the primary control over observed patterns in GSL_R, a pattern similar that shown by Fisher *et al* (2007) in Providence RI and supporting recent work indicating that urban form determines the spatial extext of urban impacts on the thermal environment (Yang *et al* 2016). The city of Madison extends ~6.5 km south from the city center, and ~8–11 km on the east and west sides of town; therefore, the radial interval from ~6.5 to 11 km distance represents the urban–rural transition zone. This transition is evident in figure 4(f), where we can see a decrease in GSL_R over this approximate interval, and relatively static baseline rural GSL_R at distances greater than 11 km. The decrease in GSL_R over this urban–rural transition zone can be explained by two mechanisms. First, this transition is characterized by a decrease in impervious cover with increasing distance from the city center (figure 1). Based on the observed relationship between GSL_T and impervious cover (section 3.1), the meteorological period suitable for vegetation growth is longer in urban areas with denser impervious cover and a warmer temperature regime, leading to a lower GSL_R in the surrounding rural areas. Second, urban areas are often characterized by exotic, ornamental, or invasive vegetation (McKinney 2002, Niinemets and Peñuelas 2008), including non-native evergreen plants, which may be characterized by a longer growing season (Shustack *et al* 2009, Nemec *et al* 2011). Thus, we suggest that decreases in non-native vegetation moving outward from the city center

contributes to the observed decrease in GSL_R over the urban–rural transition zone and reinforces previously described temperature effects.

3.3. Comparison between remotely sensed and temperature-based metrics

While temperature-based and remotely sensed metrics show comparable patterns of longer growing seasons in urban Madison compared to the rural surroundings, when SOS/EOS are compared directly there is no statistically significant relationship between temperature-based and remotely sensed phenology at the individual sensor level (figures 4(b) and (d); $R^2 < 0.06$). As noted in section 2.4, we did not expect there to be a 1:1 relationship between SOS_T/EOS_T (which represents the individual 2012–2014 growing seasons) and SOS_R/EOS_R (which represents the mean of the 2003–2013 growing seasons); rather, we hypothesized that there would be a significant positive correlation between the two methods due to persistent interannual temperature effects on phenology described in section 3.1, with a bias between methods due to the different sampling intervals. To study the drivers of differences between temperature-based and remotely sensed metrics, we introduced three difference metrics (SOS_{Diff}, EOS_{Diff}, GSL_{Diff}) in section 2.4. For each difference metric, a positive value indicates that remotely sensed estimates correspond to a longer growing season than would be predicted from meteorological data (e.g. $SOS_R < SOS_T$, $EOS_R > EOS_T$, and $GSL_R > GSL_T$).

We find significant relationships between our different metrics and the land cover in the area surrounding each sensor (figure 5). Relationships between impervious cover (%I) and our difference metrics are best explained by a piecewise linear function, with a breakpoint determined as the %I which minimizes the sum of squared errors between model fit and difference metrics. Breakpoints are consistent across difference metrics at %I of 35% (SOS_{Diff}), 37% (EOS_{Diff}), and 36% (GSL_{Diff}) (figure 5). Beneath this breakpoint, increasing %I is associated with a longer realized growing season relative to meteorological potential at a rate of 6.5 d/10%, with approximately even contributions from changes to SOS_{Diff} and EOS_{Diff}. Above this breakpoint, increasing %I is associated with a shorter growing season at a rate of 4.1 d/10%, with ~2 times stronger effects on EOS_{Diff} than SOS_{Diff}.

We attribute this piecewise pattern to two drivers: vegetation composition and urban stress regimes. First, moving outward from the city center, land cover transitions between the following classes: (Zone 1) high-density urban areas dominated by impervious cover, to (Zone 2) old neighborhoods with a thick urban canopy dominated by tree cover, to (Zone 3) recently developed areas with sparse urban canopies and a stronger grass signal, to (Zone 4) rural areas predominantly characterized by agriculture and trees (figures 1(c)–(e)). Sensors with peak difference metrics (30% < %I < 40%) are primarily in low-density urban areas (Zone 3) surrounding Madison, as well as outlying towns and villages, where grass cover is highest, and the other sensors making up the increasing limb (%I < 36%) are in rural areas or the urban outskirts (Zone 4), where most remaining natural vegetation is trees. Therefore, the increasing limb of the %I relationships represents an increase in the relative proportion of cold-tolerant urban turfgrass within vegetated areas (%G), which is typically green from shortly after snowmelt in the spring until the first winter snowfall, moving from Zone 4 into Zone 3. This is supported by a significant positive correlation between %G and SOS_{Diff} ($R^2 = 0.24$, $p < 0.001$), as well as a weakly positive correlation with EOS_{Diff} ($R^2 = 0.02$, $p < 0.05$) (figure 5). Overall, GSL_{Diff} increases (i.e. the observable period of greenness grows longer relative to our temperature-based estimates) by 2 d for every 10% increase in %G, with ~75% of that change occurring at the beginning of the growing season. The decreasing limb of the %I relationships, then, may also be partially explained by the decrease in grass cover associated with the transition from low-density urban areas surrounding Madison (Zone 3) to the higher-density areas closer to the city center (Zones 1 and 2) in which %G decreases.

Second, we suggest that the decreasing limb observed in %I relationships is may be due to increased water or pollutant stress in denser urban areas (Zones 1 and 2), which can lead to early onset of senescence and effectively decouples EOS_R from meteorological conditions (Gratani *et al* 2000, Honour *et al* 2009, Sjoman and Nielsen 2010). This is supported by the observation that the slope of the decreasing relationship between %I and EOS_{Diff} is approximately double the slope of the decreasing relationship between %I and SOS_{Diff}. While our analysis does not consider irrigation, variability in water available to plants as a result of urban irrigation (e.g. Pataki *et al* 2011, Bijoor *et al* 2012, Vico *et al* 2014) may further decouple EOS_R from EOS_T, e.g. by allowing irrigated vegetation to remain green during drought while non-irrigated vegetation may senesce.

While our analysis is conducted at a plant functional type level (e.g. grass versus trees), previous field- and plot-based studies have shown that phenological response to temperature varies at the species level (Bradley *et al* 1999, Chuine 2000, Primack *et al* 2004, Morin *et al* 2009, Vitasse *et al* 2009, Jochner *et al* 2013). A further complication is that non-native vegetation is common to urban areas and may be associated with earlier greening in the spring and a concomitantly longer GSL_R, as discussed in section 3.2 (McKinney 2002, Niinemets and Peñuelas 2008, Shustack *et al* 2009, Nemec *et al* 2011). If we assume that non-native vegetation common to urban areas has a longer growing season than native vegetation, this would cause an earlier SOS_T (*downward* shift of urban

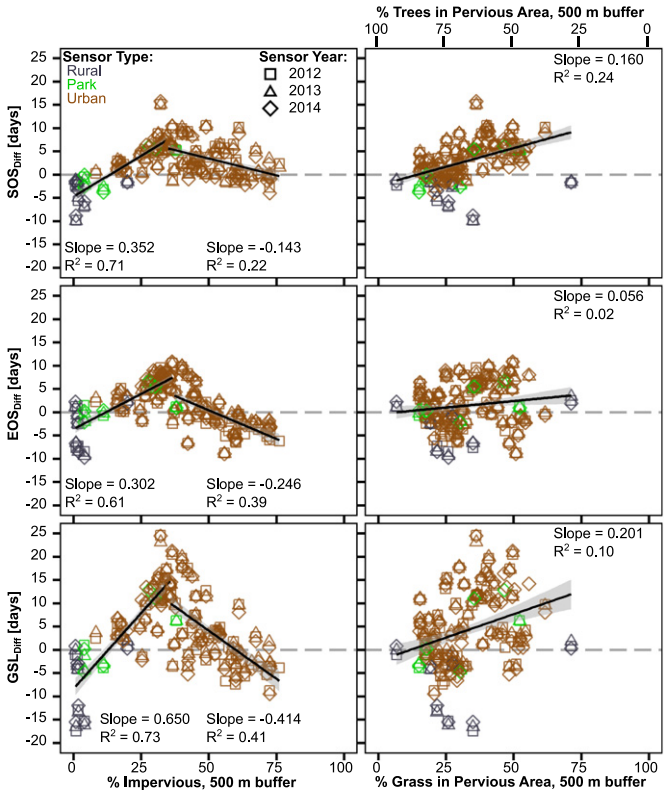

Figure 5. Comparison of the difference metrics with land cover within a 500 m buffer of each sensor estimated using the hybrid method. Positive values on *y* axis indicate that the remotely sensed predictions of GSL are longer than the temperature threshold estimates. In right set of plots, % Grass and % Trees in Pervious Area must add up to 100 and reported slopes are based on % Grass. Plots exclude sensors with >75% masked pixels within a 500 m buffer. All relationships are statistically significant at $p < 0.05$.

sensors in figure 4(b)) and a later EOS_T (*upward* shift of urban sensors in figure 4(d)), both of which would improve the correlation between temperature-based and remotely sensed phenological metrics.

While our temperature-based method accounts for potential variability in species-specific biological responses to thermal conditions by varying input parameters to our HDD/CDD equations (see appendix S1), this technique implicitly assumes a random and homogeneous distribution of all species by equally weighting all parameter combinations when calculating the mean SOS_T/EOS_T for each sensor. To account for spatial variability in species composition, the fitting parameters in table S1 could be 'tuned' to maximize agreement between SOS_T/SOS_R and EOS_T/EOS_R at each sensor (e.g. Fisher *et al* 2007); however, this approach would assume that temperature is the only factor contributing to spatial variability in phenology, whereas factors such as intra-species variability in response to photoperiod or environmental stressors may contribute to spatial variability in phenology (Gratani *et al* 2000, Saxe *et al* 2001, Schaber and Badeck 2003, Honour *et al* 2009, Caffarra *et al* 2011). Urban pixels are typically mixes of the built environment and vegetation (Gao *et al* 2006, Klosterman *et al* 2014, Lazzarini *et al* 2015, Walker *et al* 2015), leading to greater variability in both land cover and phenology than natural areas (Buyantuyev and Wu 2012).

These results provide the first synthesis of remotely sensed phenology with a dense ground-based urban temperature sensor network, and highlight a disagreement between the two methods which is associated with fine-scale variability in land cover. As previous work has reported substantial bias between remotely sensed and observed phenology, SOS_R/EOS_R are typically used to compare the relative timing of phenological events, rather than the exact dates (White *et al* 2009, Cong *et al* 2012, Xu *et al* 2014). However, here we show that remotely sensed observations of variability in land surface phenology cannot be used as a proxy for UHI intensity, as the vegetative response to meteorological conditions is dependent on the highly variable land cover at and surrounding a point. Even when focusing on the response of a single plant functional type to the UHI, such as forests in Fisher *et al* (2006) and Elmore *et al* (2012), we find that land cover (particularly %I) surrounding a pixel alters realized GSL and needs to be considered before conclusions can be drawn about the strength of the UHI. These results extend previous work done at larger spatial scales showing a disconnect between meteorological conditions and phenological response (Fisher *et al* 2007) and indicates that local processes, particularly land cover composition, must be considered as an important control over the vegetative response to

changes in land cover in addition to changes in climate.

4. Conclusions

Overall, we find that the UHI has a significant impact on urban phenology with intra-urban variability over fine spatial scales in response to local land cover composition. Across all growing seasons, we find that the UHI leads to statistically significant increases GSL_T in urban areas, with a PCI effect partially counteracting the UHI impacts on GSL_T and a small and relatively localized lake effect near the lakeshore (figure 2). Impervious cover in the area surrounding temperature sensors explains ~50%–70% of observed variability in both SOS_T and EOS_T (figure 3). However, the magnitude of the UHI impact on phenology varies interannually, and is driven by the prevailing regional weather conditions during the spring/fall transitional seasons. As such, we conclude that studies based on a single year of data are likely not generalizable to other growing seasons, though spatial patterns are likely to be consistent across years.

Comparison between remotely sensed and temperature-based phenology reveals that there is no relationship between remotely sensed and temperature-based SOS, EOS, or GSL at the individual sensor level (figures 4(b) and (d); $R^2 < 0.06$). We attribute this to the impacts of impervious cover and vegetation type within the zone of influence surrounding each sensor on the realized phenological response to meteorological conditions. Furthermore, our results demonstrate that remotely sensed phenology cannot be used as a simple proxy for UHI intensity due to potential confounding effects of local land cover composition. These results represent a first step towards better understanding local drivers of phenological variability including environmental stressors, photoperiod, and plant species and functional type variability, which has been suggested by previous studies (Cleland *et al* 2007).

As impervious surfaces are the defining characteristic of cities worldwide and our results show that local-scale impervious cover represents the dominant control over observed intra-urban variability in phenology, we expect these process-based conclusions to be broadly applicable to other cities, particularly in temperate climates. This study represents the first comparison between temperature-based phenological estimates from an urban sensor network and remotely sensed estimates; as urban meteorological networks become more common (e.g. Smoliak *et al* 2015), future work should focus on understanding the mechanisms by which land cover influences the vegetative response to urban warming and implications of UHI-induced variability in phenology for water, energy, and nutrient cycling.

Acknowledgments

SCZ, JS, CJK, and SPL are funded by the National Science Foundation Water Sustainability & Climate Program (DEB-1038759) and the North Temperate Lakes Long-Term Ecological Research Program (DEB-0822700). PT and AS acknowledge support from the NASA Applied Science program (NNX14AC36G). Tedward Erker provided helpful discussion regarding urban vegetation. The University of Wisconsin-Madison Center for High Throughput Computing (CHTC) provided computational resources for satellite image processing. We thank our community partners for use of their streetlight and utility poles: Madison Gas & Electric (RJ Hess), Alliant Energy (Jeff Nelson), the City of Madison (Dan Dettmann), Madison City Parks (Kay Rutledge), Sun Prairie Utilities (Rick Wicklund; Karl Dahl), Waunakee Utilities (Dave Dresen), the UW-Madison Arboretum (Brad Herrick), the City of Fitchburg (Holly Powell), UW-Madison (Kurtis Johnson), and Dane County (Darren Marsh). Temperature data are available by contacting JS or CJK. We appreciate the comments of two anonymous reviewers, which significantly improved the quality of the manuscript.

References

Ault T R, Henebry G M, de Beurs K M, Schwartz M D, Betancourt J L and Moore D 2013 The false spring of 2012, earliest in North American record *EOS Trans. Am. Geophys. Union* **94** 181–2

Bijoor N S, McCarthy H R, Zhang D and Pataki D E 2012 Water sources of urban trees in the Los Angeles metropolitan area *Urban Ecosyst.* **15** 195–214

Bradley C A and Altizer S 2007 Urbanization and the ecology of wildlife diseases *Trends Ecol. Evol.* **22** 95–102

Bradley N L, Leopold A C, Ross J and Huffaker W 1999 Phenological changes reflect climate change in Wisconsin *Proc. Natl Acad. Sci. USA* **96** 9701–4

Buyantuyev A, Wu J and Gries C 2007 Estimating vegetation cover in an urban environment based on Landsat ETM+ imagery: a case study in Phoenix, USA *Int. J. Remote Sens.* **28** 269–91

Buyantuyev A and Wu J 2012 Urbanization diversifies land surface phenology in arid environments: interactions among vegetation, climatic variation, and land use pattern in the Phoenix metropolitan region, USA *Landscape Urban Plan.* **105** 149–59

Caffarra A, Donnelly A, Chuine I and Jones M B 2011 Modelling the timing of Betula pubescens budburst: I. Temperature and photoperiod: a conceptual model *Clim. Res.* **46** 147–57

Cannell M G R and Smith R I 1983 Thermal time, chill days and prediction of budburst in Picea sitchensis *J. Appl. Ecol.* **20** 951–63

Chuine I 2000 A unified model for budburst of trees *J. Theor. Biol.* **207** 337–47

Cleland E E, Chuine I, Menzel A, Mooney H A and Schwartz M D 2007 Shifting plant phenology in response to global change *Trends Ecol. Evol.* **22** 357–65

Cohen B 2006 Urbanization in developing countries: current trends, future projections, and key challenges for sustainability *Technol. Soc.* **28** 63–80

Comber A and Brunsdon C 2015 A spatial analysis of plant phenophase changes and the impact of increases in urban land use *Int. J. Climatol.* **35** 972–80

Cong N, Piao S, Chen A, Wang X, Lin X, Chen S, Han S, Zhou G and Zhang X 2012 Spring vegetation green-up date in China inferred from SPOT NDVI data: a multiple model analysis *Agric. Forest Meteorol.* **165** 104–13

Dobrowski S Z 2011 A climatic basis for microrefugia: the influence of terrain on climate *Glob. Change Biol.* **17** 1022–35

Elmore A J, Guinn S M, Minsley B J and Richardson A D 2012 Landscape controls on the timing of spring, autumn, and growing season length in mid-Atlantic forests *Glob. Change Biol.* **18** 656–74

Feyisa G L, Dons K and Meilby H 2014 Efficiency of parks in mitigating urban heat island effect: an example from Addis Ababa *Landscape Urban Plan.* **123** 87–95

Fisher J I, Mustard J F and Vadeboncoeur M A 2006 Green leaf phenology at Landsat resolution: scaling from the field to the satellite *Remote Sens. Environ.* **100** 265–79

Fisher J I, Richardson A D and Mustard J F 2007 Phenology model from surface meteorology does not capture satellite-based greenup estimations *Glob. Change Biol.* **13** 707–21

Fotiou C, Damialis A, Krigas N, Halley J M and Vokou D 2011 Parietaria judaica flowering phenology, pollen production, viability and atmospheric circulation, and expansive ability in the urban environment: impacts of environmental factors *Int. J. Biometeorol.* **55** 35–50

Fry J A, Xian G, Jin S M, Dewitz J A, Homer C G, Yang L M, Barnes C A, Herold N D and Wickham J D 2011 Completion of the 2006 national land cover database for the conterminous United States *Photogramm. Eng. Remote Sens.* **77** 858–64

Fu Y, Zhang H, Dong W and Yuan W 2014a Comparison of phenology models for predicting the onset of growing season over the Northern Hemisphere *PLoS One* **9** e109544

Fu Y H, Piao S, Op de Beeck M, Cong N, Zhao H, Zhang Y, Menzel A and Janssens I A 2014b Recent spring phenology shifts in western Central Europe based on multiscale observations *Glob. Ecol. Biogeogr.* **23** 1255–63

Gan M, Deng J, Zheng X, Hong Y and Wang K 2014 Monitoring urban greenness dynamics using multiple endmember spectral mixture analysis *PLoS One* **9** e112202

Gao F, Masek J G, Schwaller M and Hall F 2006 On the blending of the Landsat and MODIS surface reflectance: predicting daily Landsat surface reflectance *IEEE Trans. Geosci. Remote Sens.* **44** 2207–18

Gazal R, White M A, Gillies R, Rodemaker E, Sparrow E and Gordon L 2008 GLOBE students, teachers, and scientists demonstrate variable differences between urban and rural leaf phenology *Glob. Change Biol.* **14** 1568–80

Georgescu M, Mahalov A and Moustaoui M 2012 Seasonal hydroclimatic impacts of Sun Corridor expansion *Environ. Res. Lett.* **7** 034026

Georgescu M, Moustaoui M, Mahalov A and Dudhia J 2013 Summer-time climate impacts of projected megapolitan expansion in Arizona *Nat. Clim. Change* **3** 37–41

Gratani L, Crescente M F and Petruzzi C 2000 Relationship between leaf life-span and photosynthetic activity of Quercus ilex in polluted urban areas (Rome) *Environ. Pollut.* **110** 19–28

Honour S L, Bell J N B, Ashenden T W, Cape J N and Power S A 2009 Responses of herbaceous plants to urban air pollution: effects on growth, phenology and leaf surface characteristics *Environ. Pollut.* **157** 1279–86

Jeong J-H, Ho C-H, Linderholm H W, Jeong S-J, Chen D and Choi Y-S 2011 Impact of urban warming on earlier spring flowering in Korea *Int. J. Climatol.* **31** 1488–97

Jin S, Yang L, Danielson P, Homer C, Fry J and Xian G 2013 A comprehensive change detection method for updating the National Land Cover Database to circa 2011 *Remote Sens. Environ.* **132** 159–75

Jochner S, Alves-Eigenheer M, Menzel A and Morellato L P C 2013 Using phenology to assess urban heat islands in tropical and temperate regions *Int. J. Climatol.* **33** 3141–51

Jochner S and Menzel A 2015 Urban phenological studies—past, present, future *Environ. Pollut.* **203** 250–61

Jochner S C, Sparks T H, Estrella N and Menzel A 2012 The influence of altitude and urbanisation on trends and mean dates in phenology (1980–2009) *Int. J. Biometeorol.* **56** 387–94

Keenan T F *et al* 2014 Net carbon uptake has increased through warming-induced changes in temperate forest phenology *Nat. Clim. Change* **4** 598–604

Klosterman S T, Hufkens K, Gray J M, Melaas E, Sonnentag O, Lavine I, Mitchell L, Norman R, Friedl M A and Richardson A D 2014 Evaluating remote sensing of deciduous forest phenology at multiple spatial scales using PhenoCam imagery *Biogeosciences* **11** 4305–20

Lazzarini M, Molini A, Marpu P R, Ouarda T B M J and Ghedira H 2015 Urban climate modifications in hot desert cities: the role of land cover, local climate, and seasonality *Geophys. Res. Lett.* **42** 9980–9

Liang L, Schwartz M D, Wang Z, Gao F, Schaaf C B, Tan B, Morisette J T and Zhang X 2014 A cross comparison of spatiotemporally enhanced springtime phenological measurements from satellites and ground in a northern US mixed forest *IEEE Trans. Geosci. Remote Sens.* **52** 7513–26

Masek J G, Vermote E F, Saleous N, Wolfe R, Hall F G, Huemmrich F, Gao F, Kutler J and Lim T K 2006 *LEDAPS Landsat Calibration, Reflectance, Atmospheric Correction Preprocessing Code* (Oak Ridge, TN: Oak Ridge National Laboratory Distributed Active Archive Center) (doi:10.3334/ORNLDAAC/1080)

McKinney M L 2002 Urbanization, biodiversity, and conservation *BioScience* **52** 883–90

Melaas E K, Friedl M A and Zhu Z 2013 Detecting interannual variation in deciduous broadleaf forest phenology using Landsat TM/ETM + data *Remote Sens. Environ.* **132** 176–85

Menzel A and Fabian P 1999 Growing season extended in Europe *Nature* **397** 659–659

Mimet A, Pellissier V, Quenol H, Aguejdad R, Dubreuil V and Roze F 2009 Urbanisation induces early flowering: evidence from Platanus acerifolia and Prunus cerasus *Int. J. Biometeorol.* **53** 287–98

Morin X, Lechowicz M J, Augspurger C, O' Keefe J, Viner D and Chuine I 2009 Leaf phenology in 22 North American tree species during the 21st century *Glob. Change Biol.* **15** 961–75

Neil K L, Landrum L and Wu J 2010 Effects of urbanization on flowering phenology in the metropolitan Phoenix region of USA: findings from herbarium records *J. Arid Environ.* **74** 440–4

Nemec K T, Allen C R, Alai A, Clements G, Kessler A C, Kinsell T, Major A and Stephen B J 2011 Woody invasions of urban trails and the changing face of urban forests in the Great Plains, USA *Am. Midland Naturalist* **165** 241–56

Niinemets Ü and Peñuelas J 2008 Gardening and urban landscaping: significant players in global change *Trends Plant Sci.* **13** 60–5

Oke T R 1973 City size and the urban heat island *Atmos. Environ.* **7** 769–79

Oke T R 1982 The energetic basis of the urban heat island *Q. J. R. Meteorol. Soc.* **108** 1–24

Oke T R 1988 The urban energy balance *Prog. Phys. Geogr.* **12** 471–508

Oke T R 2006 Initial guidance to obtain representative meteorological observations at urban sites *Instruments and Observing Methods Report No.* World Meteorological Organization WMOTD 1250

Omoto Y and Aono Y 1990 Estimation of change in blooming dates of cherry flower by urban warming *J. Agric. Meteorol.* **46** 123–30

Orsini F, Kahane R, Nono-Womdim R and Gianquinto G 2013 Urban agriculture in the developing world: a review *Agronomy Sustainable Dev.* **33** 695–720

Pataki D E, McCarthy H R, Litvak E and Pincetl S 2011 Transpiration of urban forests in the Los Angeles metropolitan area *Ecol. Appl.* **21** 661–77

Penuelas J, Rutishauser T and Filella I 2009 Phenology feedbacks on climate change *Science* **324** 887–8

Primack D, Imbres C, Primack R B, Miller-Rushing A J and Del Tredici P 2004 Herbarium specimens demonstrate earlier flowering times in response to warming in Boston *Am. J. Bot.* **91** 1260–4

Richardson A D, Bailey A S, Denny E G, Martin C W and O'Keefe J 2006 Phenology of a northern hardwood forest canopy *Glob. Change Biol.* **12** 1174–88

Richardson A D, Keenan T F, Migliavacca M, Ryu Y, Sonnentag O and Toomey M 2013 Climate change, phenology, and phenological control of vegetation feedbacks to the climate system *Agric. Forest Meteorol.* **169** 156–73

Roetzer T, Wittenzeller M, Haeckel H and Nekovar J 2000 Phenology in central Europe—differences and trends of spring phenophases in urban and rural areas *Int. J. Biometeorol.* **44** 60–6

Saxe H, Cannell M G R, Johnsen B, Ryan M G and Vourlitis G 2001 Tree and forest functioning in response to global warming *New Phytol.* **149** 369–99

Schaber J and Badeck F W 2003 Physiology-based phenology models for forest tree species in Germany *Int. J. Biometeorol.* **47** 193–201

Schatz J and Kucharik C J 2014 Seasonality of the urban heat island effect in Madison, Wisconsin *J. Appl. Meteorol. Climatol.* **53** 2371–86

Schatz J and Kucharik C J 2015 Urban climate effects on extreme temperatures in Madison, Wisconsin, USA *Environ. Res. Lett.* **10** 094024

Schatz J and Kucharik C J 2016 Urban heat island effects on growing seasons and heating and cooling degree days in Madison, Wisconsin USA *Int. J. Climatol.* in press (doi:10.1002/joc.4675)

Schmidlin T 1989 The Urban Heat-Island at Toledo, Ohio *Ohio J. Sci.* **89** 38–41

Schwartz M D and Marotz G A 1986 An approach to examining regional atmosphere-plant interactions with phenological data *J. Biogeogr.* **13** 551–60

Schwartz M D and Reiter B E 2000 Changes in North American spring *Int. J. Climatol.* **20** 929–32

Serbin S P, Singh A, McNeil B E, Kingdon C C and Townsend P A 2014 Spectroscopic determination of leaf morphological and biochemical traits for northern temperate and boreal tree species *Ecol. Appl.* **24** 1651–69

Shustack D P, Rodewald A D and Waite T A 2009 Springtime in the city: exotic shrubs promote earlier greenup in urban forests *Biol. Invasions* **11** 1357–71

Sjoman H and Nielsen A B 2010 Selecting trees for urban paved sites in Scandinavia—a review of information on stress tolerance and its relation to the requirements of tree planners *Urban Forestry Urban Greening* **9** 281–93

Small C 2001 Estimation of urban vegetation abundance by spectral mixture analysis *Int. J. Remote Sens.* **22** 1305–34

Smoliak B V, Snyder P K, Twine T E, Mykleby P M and Hertel W F 2015 Dense network observations of the Twin Cities canopy-layer urban heat island *J. Appl. Meteorol. Climatol.* **54** 1899–917

Spronken-Smith R A and Oke T R 1999 Scale modelling of nocturnal cooling in urban parks *Bound.-Layer Meteorol.* **93** 287–312

Spronken-Smith R A, Oke T R and Lowry W P 2000 Advection and the surface energy balance across an irrigated urban park *Int. J. Climatol.* **20** 1033–47

Stagoll K, Lindenmayer D B, Knight E, Fischer J and Manning A D 2012 Large trees are keystone structures in urban parks *Conservation Lett.* **5** 115–22

Taha H, Akbari H and Rosenfeld A 1991 Heat island and oasis effects of vegetative canopies: micro-meteorological field-measurements *Theor. Appl. Climatol.* **44** 123–38

Thebo A L, Drechsel P and Lambin E F 2014 Global assessment of urban and peri-urban agriculture: irrigated and rainfed croplands *Environ. Res. Lett.* **9** 114002

Todhunter P E 1996 Environmental indices for the Twin Cities Metropolitan Area (Minnesota, USA) urban heat island—1989 *Clim. Res.* **6** 59–69

Upmanis H and Chen D 1999 Influence of geographical factors and meteorological variables on nocturnal urban-park temperature differences-a case study of summer 1995 in Göteborg, Sweden *Clim. Res.* **13** 125–39

US Census Bureau 2010 Census urban areas (https://census.gov/geo/reference/ua/urban-rural-2010.html) (accessed 25 March 2015)

Vico G, Revelli R and Porporato A 2014 Ecohydrology of street trees: design and irrigation requirements for sustainable water use *Ecohydrology* **7** 508–23

Vitasse Y, Delzon S, Dufrene E, Pontailler J-Y, Louvet J-M, Kremer A and Michalet R 2009 Leaf phenology sensitivity to temperature in European trees: do within-species populations exhibit similar responses? *Agric. Forest Meteorol.* **149** 735–44

Walker J J, de Beurs K M and Henebry G M 2015 Land surface phenology along urban to rural gradients in the US Great Plains *Remote Sens. Environ.* **165** 42–52

Walker J J, de Beurs K M, Wynne R H and Gao F 2012 Evaluation of Landsat and MODIS data fusion products for analysis of dryland forest phenology *Remote Sens. Environ.* **117** 381–93

Weng Q 2012 Remote sensing of impervious surfaces in the urban areas: requirements, methods, and trends *Remote Sens. Environ.* **117** 34–49

White M A *et al* 2009 Intercomparison, interpretation, and assessment of spring phenology in North America estimated from remote sensing for 1982–2006 *Glob. Change Biol.* **15** 2335–59

White M A, Nemani R R, Thornton P E and Running S W 2002 Satellite evidence of phenological differences between urbanized and rural areas of the Eastern United States deciduous broadleaf forest *Ecosystems* **5** 260–73

Wu C 2004 Normalized spectral mixture analysis for monitoring urban composition using ETM plus imagery *Remote Sens. Environ.* **93** 480–92

Wu C and Murray A T 2003 Estimating impervious surface distribution by spectral mixture analysis *Remote Sens. Environ.* **84** 493–505

Xian G, Homer C, Demitz J, Fry J, Hossain N and Wickham J 2011 Change of impervious surface area between 2001 and 2006 in the conterminous United States *Photogramm. Eng. Remote Sens.* **77** 758–62

Xu H, Twine T E and Yang X 2014 Evaluating remotely sensed phenological metrics in a dynamic ecosystem model *Remote Sens.* **6** 4660–86

Yang L, Niyogi D, Tewari M, Aliaga D, Chen F, Tian F and Ni G 2016 Contrasting impacts of urban forms on the future thermal environment: example of Beijing metropolitan area *Environ. Res. Lett.* **11** 034018

Yu C and Hien W N 2006 Thermal benefits of city parks *Energy Build.* **38** 105–20

Zhang P, Bounoua L, Imhoff M L, Wolfe R E and Thome K 2014 Comparison of MODIS land surface temperature and air temperature over the continental USA meteorological stations *Can. J. Remote Sens.* **40** 110–22

Zhang W, Li A, Jin H, Bian J, Zhang Z, Lei G, Qin Z and Huang C 2013 An enhanced spatial and temporal data fusion model for fusing Landsat and MODIS surface reflectance to generate high temporal Landsat-like data *Remote Sens.* **5** 5346–68

Zhang X, Friedl M A, Schaaf C B, Strahler A H, Hodges J C F, Gao F, Reed B C and Huete A 2003 Monitoring vegetation phenology using MODIS *Remote Sens. Environ.* **84** 471–5

Zhang X, Friedl M A, Schaaf C B, Strahler A H and Schneider A 2004 The footprint of urban climates on vegetation phenology *Geophys. Res. Lett.* **31** L12209

Zhu Z and Woodcock C E 2012 Object-based cloud and cloud shadow detection in Landsat imagery *Remote Sens. Environ.* **118** 83–94

Zipper S C and Loheide S P 2014 Using evapotranspiration to assess drought sensitivity on a subfield scale with HRMET, a high resolution surface energy balance model *Agric. Forest Meteorol.* **197** 91–102